Chemistry–A European Journal
Research Article
doi.org/10.1002/chem.202301855
Chemistry Europe
European Chemical Societies Publishing
www.chemeurj.org

# Next Generation of Fluorometric Protease Assays: 7-Nitrobenz-2-oxa-1,3-diazol-4-yl-amides (NBD-Amides) as Class-Spanning Protease Substrates

Hannah Maus[+],[a] Patrick Müller[+],[a] Mergim Meta,[a] Sabrina N. Hoba,[a] Stefan J. Hammerschmidt,[a] Robert A. Zimmermann,[a] Collin Zimmer,[a] Natalie Fuchs,[a] Tanja Schirmeister,[a] and Fabian Barthels*[a]

Fluorometric assays are one of the most frequently used methods in medicinal chemistry. Over the last 50 years, the reporter molecules for the detection of protease activity have evolved from first-generation colorimetric *p*-nitroanilides, through FRET substrates, and 7-amino-4-methyl coumarin (AMC)-based substrates. The aim of further substrate development is to increase sensitivity and reduce vulnerability to assay interferences. Herein, we describe a new generation of substrates for protease assays based on 7-nitrobenz-2-oxa-1,3-diazol-4-yl-amides (NBD-amides). In this study, we synthesized and tested substrates for 10 different proteases from the serine-, cysteine-, and metalloprotease classes. Enzyme- and substrate-specific parameters as well as the inhibitory activity of literature-known inhibitors confirmed their suitability for application in fluorometric assays. Hence, we were able to present NBD-based alternatives for common protease substrates. In conclusion, these NBD substrates are not only less susceptible to common assay interference, but they are also able to replace FRET-based substrates with the requirement of a prime site amino acid residue.

## Introduction

Fluorescence is one manifestation of the interaction of electromagnetic radiation with matter which is ubiquitously used for the analysis of all kinds of parameters in the life sciences.[1] It is widely used for the characterization of protein structures and protein/ligand interactions.[2] This comprises the analysis of protein structural changes, localization of proteins in cells, organisms, and the determination of binding affinities between proteins and their ligands.[3–6] Proteolytic enzymes represent a current field of research, because of their mechanistic involvement in many diseases from virus infections to cancer progression and immunological disorders.[7–9] Since 1964, more than 64 protease inhibitors were approved by the Food and Drug Administration (FDA) for application in human therapies;[10,11] exemplarily, the recently approved cysteine protease inhibitor Nirmatrelvir is being used to treat the SARS-CoV 2 infection.[12] This implies, that proteases are still important targets, and the scientific community strives for discovering new protease-targeting drugs.[13,14]

Due to their time efficiency and steadily growing supply of commercially available fluorogenic protease substrates, fluorometric assays are one of the most frequently used methods in medicinal chemistry to analyze protease-inhibiting drug candidates.[15,16] The first, in 1973 introduced fluorogenic substrates used for the measurement of protease activities were FRET-based (Förster resonance energy transfer) substrates which harbor a quencher and fluorophore molecular pair (Figure 1).[17] These replaced the previously utilized colorimetric *p*-nitroanilide (pNA) substrates, because of their higher detection sensitivity.[18] Only a few years later, in 1976, the corresponding amides of a fluorescent coumarin derivative (7-amino-4-methyl coumarin, AMC) were implemented as a new fluorogenic protease substrate which decreased the vulnerability to assay interferences compared to the FRET-based and colorimetric pNA substrates.[19]

In general, the principle of fluorometric protease assays is described as follows: The target enzyme cleaves an amide bond of the substrate, which leads to a change in fluorescence properties of the fluorogenic reporter, for example by separation of the quencher from the fluorophore (FRET substrate) or cleavage of the internally quenched fluorogenic residue from the substrate (AMC substrate).[20] The fluorophore is then excited within a cuvette fluorometer or a microplate reader at a specific excitation wavelength and the resulting fluorescence can be detected at its corresponding emission wavelength. The increasing fluorescence intensity over time describes a scale of enzymatic activity. By the addition of an inhibitor, the reaction rate of the enzyme is attenuated which gives information about the inhibitory activity by different evaluation methods. How-

[a] H. Maus,[+] P. Müller,[+] M. Meta, S. N. Hoba, S. J. Hammerschmidt, R. A. Zimmermann, C. Zimmer, N. Fuchs, Prof. Dr. T. Schirmeister, Dr. F. Barthels
Institute of Pharmaceutical and Biomedical Sciences
Johannes Gutenberg-University
Staudingerweg 5, 55128 Mainz (Germany)
E-mail: barthels@uni-mainz.de
Homepage: https://ak-barthels.pharmazie.uni-mainz.de/
[+] These authors contributed equally to this manuscript.

Supporting information for this article is available on the WWW under https://doi.org/10.1002/chem.202301855

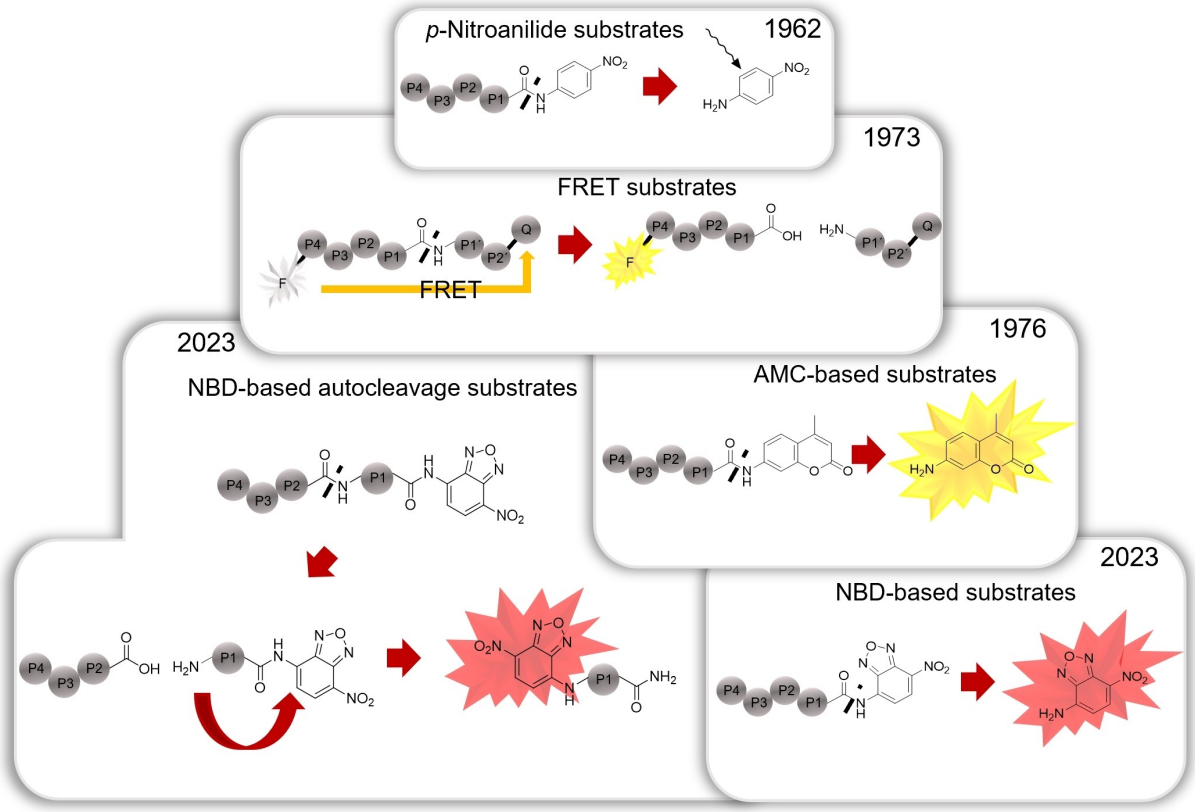


**Figure 1.** Timeline of protease substrates development with selected example substrates including *p*-nitroanilides (first described in 1962), FRET- (1973), and AMC-based (1976) fluorogenic substrates. In this study, we report the development of newly designed NBD-based protease substrates for biochemical and medicinal chemistry assays.

ever, not less important is the resilience of a fluorometric assay system regarding non-specific interference effects, that originate from various sources of errors like assay components, including the analyzed drug compounds themselves.[21–23] Assay interferences lead to both false positive and false negative results, which makes it necessary to validate potential hits with an additional, orthogonal methodology.[24]

A known strategy for mitigation of intrinsic assay interferences is based on the fact that many of the interfering physicochemical transitions do occur in the near UV-light spectrum, due to the molecular properties of mostly aromatic drug-like inhibitors.[25] One option to avoid inhibitor-induced interferences is to shift the assay wavelengths to the lower-energy range of light, and hence, there are existing biochemical methods using fluorescent dyes (BODIPY, Cy5, etc.) with their excitation and emission maxima in the red wavelength region (> 580 nm), leading to minimized interferences.[26,27] Over the last 30 years, FRET substrates were optimized by an overall shift to longer wavelengths like Dabcyl/EDANS resulting in optimized sensitivity, photochemical, and low-interference properties.[28] In contrast to the most frequently used AMC- ($\lambda_{ex} = 380$ nm, $\lambda_{em} = 460$ nm) and FRET-based (Dabcyl/EDANS; $\lambda_{ex} = 340$ nm, $\lambda_{em} = 490$ nm) fluorogenic substrates, the 4-amino-7-nitrobenzofurazane (NBD) fluorophore displays excitation and emission maxima in the fluorescein wavelength magnitude ( $\lambda_{ex} = 485$ nm, $\lambda_{em} = 535$ nm) and might consequently avoid common interferences associated with AMC and EDANS fluorophores.[17,19,29–31]

Applications for NBD-based chemosensors have already been described in the literature, leading to several hundreds of publications and the development of numerous commercial probes which have already been summarized in reviews.[32] For the analysis of enzymatic turnover, however, the use of NBD-based derivates has been only described for the study of histone acetyltransferases, deacetylases, and esterases.[33–37] To expand the scope, herein, we report the synthesis and characterization of peptide-based NBD-amides as substrates for various protease targets. Additionally, due to the observed Smiles rearrangement mechanism of selected NBD derivates, we were able to design substrates suited as corresponding FRET substrate alternatives (Figure 1).[38,39]

To evaluate the substrate affinity and turnover rate of the NBD-based substrates, we determined $K_M$ and $k_{cat}$ values. Both substrate benchmarks were compared with the corresponding literature known, AMC- or FRET-derived parent substrates. To demonstrate that this new assay protocol provides comparable results to the literature-described assays, $K_i$ values were determined for model inhibitors known from the literature. Afterward, the mitigation of common assay interferences of conventional fluorogenic substrates was investigated by comparing a NBD-based substrate with its AMC-based counterpart.

## Results and Discussion

### Synthesis

All NBD substrates were prepared in a two-step synthetic procedure. First, the variable peptide sequences **2a–j** spanning from the P2-site to the *N*-capped terminus were synthesized following a standard fluorenylmethoxycarbonyl (Fmoc)-solid phase peptide synthesis (SPPS) protocol using a 2-chlorotrityl resin.[40]

The second step in the synthetic sequence was the preparation of the fluorogenic reporter group through a nucleophilic aromatic substitution of precursor **3** in a methanolic ammonia solution.[41] Subsequently, the NBD amine **4** was coupled with the respective *tert*-butoxycarbonyl (Boc)-protected P1 amino acid **5**, using the *in situ* activating agents *O*-(7-azabenzotriazol-1-yl)-*N*,*N*,*N*′,*N*′-tetramethyluronium-hexafluorophosphate (HATU) or benzotriazole-1-yl-oxytripyrrolidinophosphonium-hexafluorophosphate (PyBOP), and the organic base *N*,*N*-diisopropylethylamine (DIEA). The amino group of the intermediate **6a–d** was deprotected by trifluoroacetic acid, and subsequently, coupled with the remaining peptide sequence **2** to yield the desired fluorogenic substrates **7a–j** (Scheme 1, Table 1).

### Kinetic Characterization of NDB-based Substrates

To verify and analyze the suitability of the proposed NBD-based substrates for fluorometric protease assays, the enzyme kinetic parameters $K_m$, $v_{max}$, $k_{cat}$, and the catalytic efficiency $k_{cat}/K_M$ were determined for both the NBD substrates and their corresponding parent substrates. Proteolytic cleavage of the substrate release was detected in 96-well plate format (typically 200 μL). NBD substrates were excited at 485 nm, and the emission was detected at 535 nm.[42,43] The increase in fluorescence intensity over time (reaction rate) is a measure of the activity of the protease, and thus, the fluorescent progress traces follow the Michaelis Menten equation (Eq. (1)) which was used for enzyme kinetic analysis:

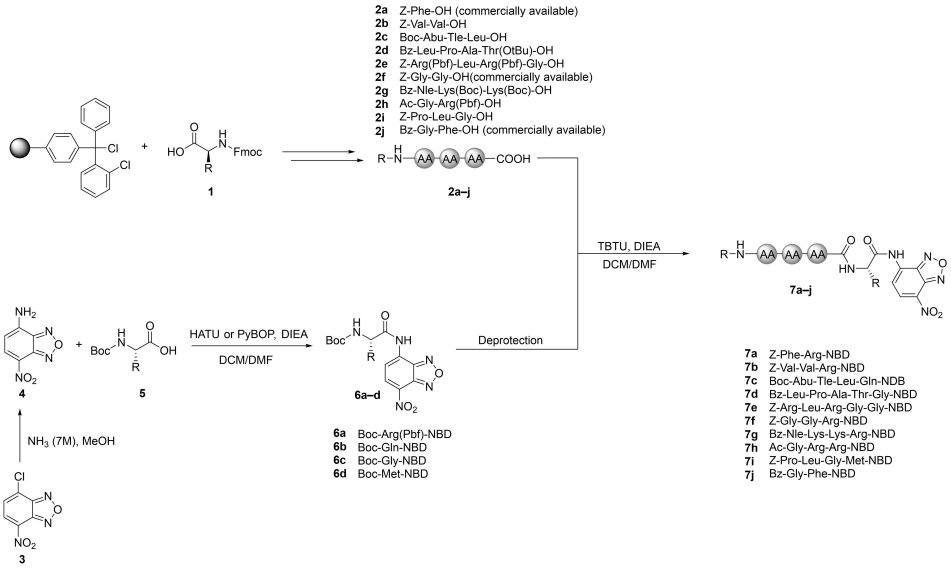


**Scheme 1.** SPPS/solution phase synthesis of the NBD-based substrates suited for cysteine-, serine-, and metalloproteases.

**Table 1.** Synthesized NBD-based substrates and their corresponding AMC-/FRET-based parent substrates.

| Protease | Protease class | NBD-based substrate | Reference/parent substrate |
|---|---|---|---|
| *T. brucei* rhodesain | Cysteine | Z–Phe–Arg–NBD (**7a**) | Z–Phe–Arg–AMC[44] |
| Cathepsin S (human) | Cysteine | Z–Val–Val–Arg–NBD (**7b**) | Z–Val–Val–Arg–AMC[45] |
| SARS-CoV 2 $M^{pro}$ | Cysteine | Boc–Abu–Tle–Leu–Gln–NBD (**7c**) | Boc–Abu–Tle–Leu–Gln–AMC[46] |
| *S. aureus* SrtA | Cysteine | Bz–Leu–Pro–Ala–Thr–Gly–NBD (**7d**) | Abz–Leu–Pro–Glu–Thr–Gly–Dap(Dnp)–OH[47] |
| SARS-CoV 2 $PL^{pro}$ | Cysteine | Z–Arg–Leu–Arg–Gly–Gly–NBD (**7e**) | Z–Arg–Leu–Arg–Gly–Gly–AMC[48] |
| uPA (human) | Serine | Z–Gly–Gly–Arg–NBD (**7f**) | Z–Gly–Gly–Arg–AMC[49] |
| DENV NS2B/NS3 | Serine | Bz–Nle–Lys–Lys–Arg–NBD (**7g**) | Bz–Nle–Lys–Lys–Arg–AMC[50] |
| ZIKV | | Ac–Gly–Arg–Arg–NBD (**7h**) | Ac–Gly–Arg–Arg–AMC[51] |
| MMP9 (human) | Metallo | Z–Pro–Leu–Gly–Met–NBD (**7i**) | Dnp–Pro–Leu–Gly–Met–Trp–Ser–Arg–$NH_2$[52] |
| Thermolysin | Metallo | Bz–Gly–Phe–NBD (**7j**) | *N*-[3-(2-furyl)acryloyl]-glycyl–L-leucine amide (FAGLA)[53,54] |

$$v_0 = \frac{v_{max} \cdot [S]}{K_M + [S]} \quad (1)$$

where $v_0$ is the initial reaction rate, at a given substrate concentration [*S*]. $v_{max}$ is the maximum reaction rate, while $K_M$ indicates [*S*] at which the conversion rate is half-maximal.

The fluorescence progress curves were acquired for at least six different substrate concentrations for the corresponding substrate with at least a technical triplicate. $K_M$ and $v_{max}$ values were then calculated from the respective Michaelis–Menten curves (Table 2 and Figures S55–S63). Exemplarily, fluorescence progress curves for different substrate concentrations and the resulting Michaelis–Menten plot are shown for the cysteine protease rhodesain in Figure 2. The signal-to-noise ratio, as described by the detector-independent reaction rate slope ([au·s$^{-1}$] vs. [*S*]), was ~3 times higher for NBD than for AMC-based substrates (calculated by the gain factor-independent initial slope of Figure 2C vs. 2D). Consequently, the NBD-based fluorescence assays can be performed at lower enzyme and/or substrate concentrations than with the corresponding parent

**Table 2.** Enzyme- and substrate-specific kinetic constants for NBD-based and corresponding AMC-based substrates. Michaelis–Menten constant ($K_M$), maximum turnover rate ($v_{max}$), turnover number ($k_{cat}$), catalytic efficiency ($k_{cat}/K_M$).

| protease | NBD substrate | | | | AMC substrate | | | |
|---|---|---|---|---|---|---|---|---|
| | $K_M$ [μM] | $v_{max}$ [nM·min$^{-1}$] | $k_{cat}$ [min$^{-1}$] | $k_{cat}/K_M$ [L·μmol$^{-1}$ min$^{-1}$] | $K_M$ [μM] | $v_{max}$ [nM·min$^{-1}$] | $k_{cat}$ [min$^{-1}$] | $k_{cat}/K_M$ [L·μmol$^{-1}$ min$^{--1}$] |
| Rhodesain | 2.84 ± 0.22 | 73.8 ± 2.6 | 59.0 ± 2.1 | 20.8 ± 1.8 | 3.08 ± 0.41 | 679 ± 43 | 1056 ± 66 | 343 ± 50 |
| uPA | 10.2 ± 0.63 | 174 ± 6 | [a] | [b] | 347 ± 35 | 1847 ± 90 | [c] | [d] |
| CatS | 28.0 ± 2.68 | 70.0 ± 3.1 | 7.00 ± 0.31 | 0.25 ± 0.03 | 34.4 ± 3.06 | 111 ± 23 | 0.45 ± 0.09 | 0.013 ± 0.003 |
| DENV NS2B/NS3 | 88.1 ± 11.7 | 762 ± 37 | 3.05 ± 0.15 | 0.035 ± 0.005 | 869 ± 67 | 41.8 ± 1.9 | 0.17 ± 0.01 | (1.92 ± 0.17) $10^{-4}$ |
| ZIKV NS2B/NS3 | 33.6 ± 1.51 | 252 ± 5 | 10.1 ± 0.2 | 0.30 ± 0.01 | 1381 ± 371 | 161 ± 34 | 1.29 ± 0.27 | (9.3 ± 3.3) $10^{-4}$ |
| $PL^{pro}$ | 40.6 ± 4.11 | 151 ± 8 | 1.51 ± 0.08 | 0.037 ± 0.004 | 1332 ± 161 | 7049 ± 427 | 70.5 ± 4.3 | 0.053 ± 0.007 |
| $M^{pro}$ | 18.9 ± 1.38 | 10.9 ± 0.4 | 2.62 ± 0.09 | 0.14 ± 0.01 | 56.7 ± 11.6 | 2.06 ± 0.16 | 0.50 ± 0.04 | 0.009 ± 0.002 |

The concentration of the uPA protein in mol·L$^{-1}$ is unknown but given in units (U) by the vendor: [a] ($1.74 \cdot 10^{-5} \pm 1.20 \cdot 10^{-7}$) mol·min$^{-1}$·U$^{-1}$; [b] (1.71 ± 0.12) L·min$^{-1}$·U$^{-1}$; [c] ($1.85 \cdot 10^{-4} \pm 9.00 \cdot 10^{-6}$) mol·min$^{-1}$·U$^{-1}$; [d] (0.53 ± 0.06) L·min$^{-1}$·U$^{-1}$.

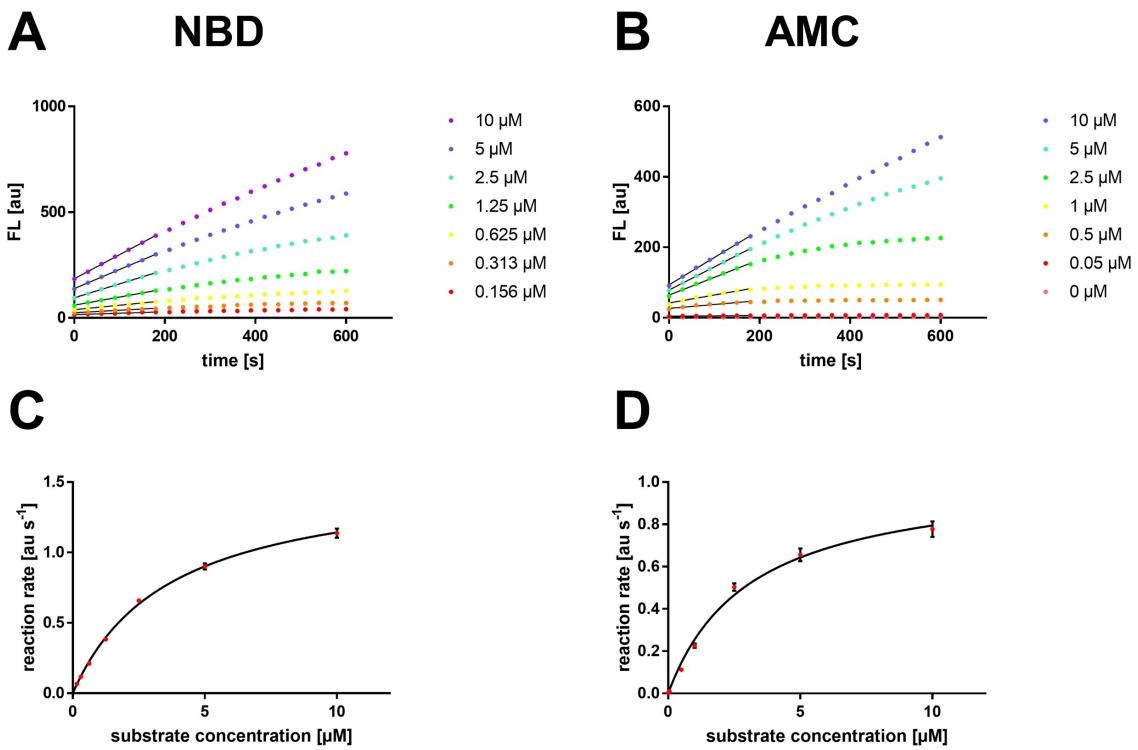


**Figure 2.** Exemplary fluorometric enzyme assay graphs for rhodesain. (A) Fluorescence progress curves for the conversion of different concentrations of the Z–Phe–Arg–NBD (7a) substrate by rhodesain. (B) Fluorescence progress curves for Z–Phe–Arg–AMC by rhodesain. (C) Michaelis–Menten plot for Z–Phe–Arg–NBD (7a). (D) Michaelis–Menten plot for Z–Phe–Arg–AMC.

substrate. Especially for highly affine ligands, this might provide an advantage to avoid tight-binding inhibition ($[E] > K_i$).[55]

In general, the $K_M$ values for the NBD-based substrates were found to be in the same order of magnitude or better than the $K_M$ values determined for the AMC-based parent substrates, indicating similar or increased affinity compared to their AMC counterpart. While the $K_M$ value of the cysteine proteases rhodesain, CatS, and $M^{pro}$ substrates is virtually unchanged by the exchange of the fluorophore from AMC to NBD, the affinity of uPA, DENV/ZIKV NS2B/NS3, and $PL^{pro}$ substrates is increased by up to a factor of ~40. The affinity increase was reasoned by analyzing the binding poses predicted by molecular docking. Comparing the docking poses of the AMC and the NBD substrate, it is noticeable that the positioning of the substrate peptide is mostly not affected by the exchange of the fluorophore residue. However, the positioning of the fluorophore itself might differ depending on the individual topology of the binding pocket. By its chemical nature, the NBD substructure can form more hydrophilic interactions compared to AMC as highlighted by the interaction analysis (Figure 3 and Figure S73). The formation of productive interactions with the charge-polarized catalytic dyad of a protease could be the reason for the improved affinity of NBD-based substrates. Some examples in which the NDB residue mediates increased affinity for protein and lipid surfaces have been previously documented.[32]

Considering the kinetics of catalytic cleavage, for the rhodesain, uPA, and $PL^{pro}$ substrates, $k_{cat}$ is lower for these NBD-based substrates than for the AMC-based substrates (10–100×). For the other enzymes, the $k_{cat}$ values are in the same magnitude or slightly higher for the NBD-based substrates. Thus, no clear trend is apparent regarding the substrate cleavage rate, which seems to be an individual characteristic for each protease probably depending on the positioning of the susceptible amide bond towards the nucleophilic enzyme residue. Except for the rhodesain substrate, the catalytic efficiency $k_{cat}/K_M$ of the NBD-based substrates was found to be as high as or higher than the one of the AMC-based substrates. In the case of the rhodesain NBD substrate (**7 a**) the reduction of the $k_{cat}$ value actually represents an advantage over the AMC substrate, since the fluorescence progress curves remain linear for a longer time in the steady-state regiment (Figure 2A) and there is no early saturation of the fluorescence by reaching an equilibrium, as is the case with the AMC substrate (Figure 2B).

## Autocleavage of a DENV and ZIKV NS2B/NS3 Protease Substrate

Remarkably, in contrast to all other substrates presented in this study, our first DENV and ZIKV NS2B/NS3 protease substrate **7 g** with the sequence Bz–Nle–Lys–Lys–Arg–NBD (Table 1) showed a fluorescence increase even in the absence of any enzyme. In an alkaline buffered solution, this fluorescence increase was found to be higher than at neutral pH values (Figure 4A and B). To analyze the molecular mechanism of this non-enzymatic fluorescence activation, the reaction mixture of the NS2B/NS3 substrate conversion was analyzed by HPLC/MS. By this, two LC peaks of the same mass (405.70 Da) but different fluorescence properties were detected, one corresponding to the substrate educt **7 g** and the other to a fluorescent product **8**, suggesting an intramolecular rearrangement mechanism for fluorescence auto-activation (Figure S49). In the literature, an intramolecular Smiles rearrangement for NBD derivatives incorporating primary amine groups has been described during a histone deacetylase assay development.[37,39]

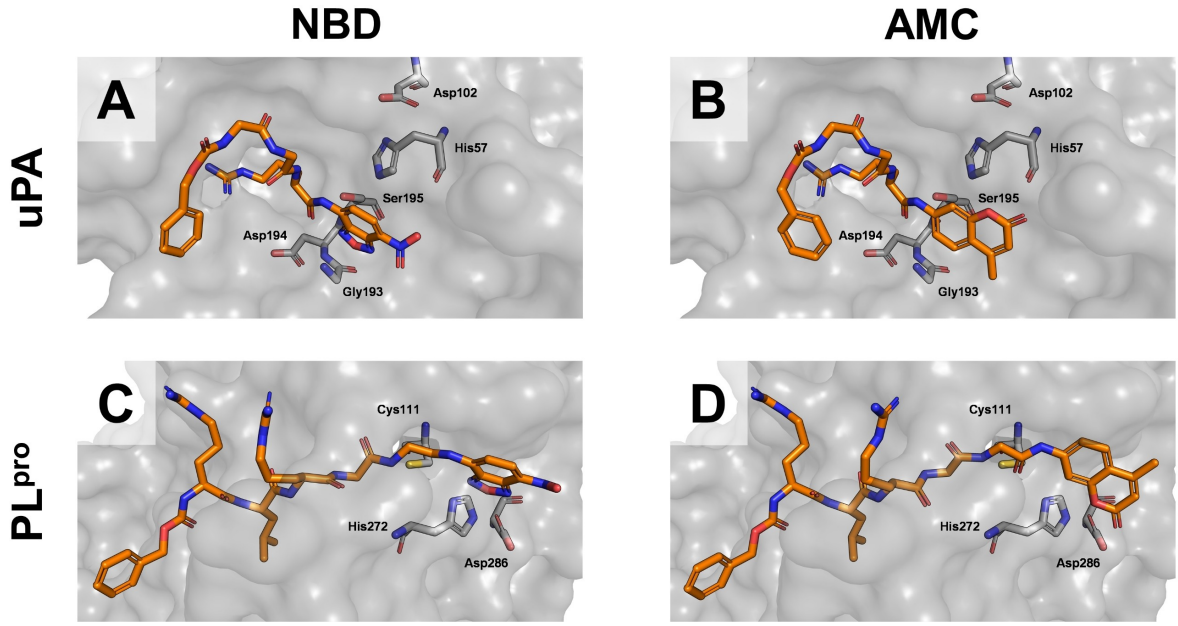


**Figure 3.** Predicted binding poses for the NBD- and AMC-based substrates for uPA and $PL^{pro}$. (A) Z–Gly–Gly–Arg–NBD (7f) in the active site of the crystal structure of uPA (pdb: 1LMW). (B) Z–Gly–Gly–Arg–AMC in the crystal structure of uPA (pdb: 1LMW). (C) Z–Arg–Leu–Arg–Gly–Gly–NBD (7e) in the crystal structure of $PL^{pro}$ (pdb: 7RBS). (D) Z–Arg–Leu–Arg–Gly–Gly–AMC in the crystal structure of $PL^{pro}$ (pdb: 7RBS).

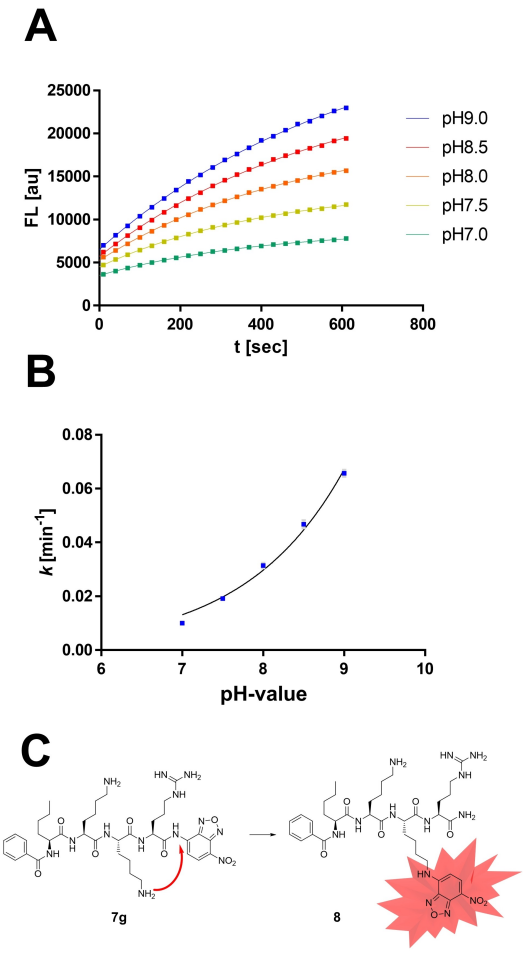


**Figure 4.** Autocleavage of the Bz–Nle–Lys–Lys–Arg–NBD (7 g) substrate. (A) Enzyme-independent fluorescence increase at different pH values (100 μM Bz–Nle–Lys–Lys–Arg–NBD in DENV NS2B/NS3 buffer). (B) pH-dependence of the non-enzymatic turnover. (C) Putative Smiles rearrangement of lysine-containing substrates.

From these and the literature results, we hypothesized that substrate auto-cleavage is enabled by the presence of free amine groups in the substrate sequence (Figure 4C). Appropriately, we found that substrates without lysine residues are stable in their respective assay buffer. This was confirmed both by mass spectroscopy and by fluorescence spectroscopy (Figures S50–S52). Nonetheless, we aimed to develop a functional substrate for the NS2B/NS3 proteases, and thus, we replaced the lysine residues with arginine residues, resulting in a stable and functional substrate for both proteases (Ac–Gly–Arg–Arg–NBD **7 h**, Table 2). Noteworthy, even high concentrations of buffers containing free amines (e.g., Tris 100 mM) do not lead to instability of the NBD substrates, however, the application scope of NBD-based substrates should be limited to lysine-free protease substrates. However, this does not represent a practical disadvantage in the development of protease substrates since there is no known protease that only tolerates lysine and not arginine.

### Harnessing NBD-Amide Autocleavage for FRET Substrate Replacement

We developed the idea of harnessing the characteristic NBD autocleavage behavior for a FRET substrate replacement (Figure 5A). By this strategy, endopeptidases with a requirement for a specific amino acid in their prime site (S1′) might also become accessible to the repertoire of NBD substrates. Such proteases that have specificity for a S1′ amino acid usually must be assayed with a matching FRET substrate because AMC substrates usually do not fulfill the S1′ specificity requirement either. To test the hypothesis if a free *N*-terminus of an $H_2N$-Xaa-NBD derivative is able to drive the Smiles rearrangement, a minimal substrate ($H_2N$–Arg(Pbf)-NBD **21 a**) was analyzed fluorometrically and by LC/MS with enzyme-free assay conditions (100 mM Tris, 100 mM NaCl, variable pH) which highlighted that fluorescence auto-activation proceeds as expected (Figure S53), while at pH value between 5 and 8 the chemical turnover rate was moderately efficient ($k = 0.01$ min$^{-1}$). Outside this pH range the Smiles rearrangement might be less efficient but at very low or high pH values most proteases do not show enzymatic activity either.

We designed several NBD substrates from commonly known FRET-based parent substrates where the *N*-terminus of the prime site (S1′) amino acid can induce a Smiles rearrangement, resulting in fluorescence increase after proteolytic cleavage and subsequent rearrangement (Figure 5A). Exemplary, such substrates were designed for the proteases SrtA (Figure 5B–C), MMP9, and thermolysin. LC/MS spectra of the enzymatic conversion can be found in the Supporting Information (Figure S54). Similar to the above-described non-prime site substrates, the NBD-based substrates for thermolysin, SrtA, and MMP9 showed similar or better affinities ($K_M$) compared to their parent substrates (Table 3). Both the turnover rates $k_{cat}$ and catalytic efficiency $k_{cat}/K_M$ of these NBD substrates were lower than those of the parent substrate. This might be explained by the two-step reaction mechanism which is limited by the second step of the chemical rearrangement with moderate efficiency. However, the disadvantage of a lower processivity will be outweighed by the higher detection sensitivity and decreased susceptibility to assay interferences (see below).

### Applications for Protease Inhibitor Investigation

To confirm the applicability of the NBD-based substrates in drug discovery-relevant fluorometric assays, the inhibition constants $K_i$ of literature-known inhibitors were determined for each protease using NBD-based and the matching parent substrates (Table S2 and Figures S64–S72). Inhibition constants ($K_i$) were determined from the fluorescence progress curves using the Cheng-Prusoff equation (Eq. (2)).[56]

$$K_i = \frac{IC_{50}}{1 + \left(\frac{[S]}{K_M}\right)} \quad (2)$$

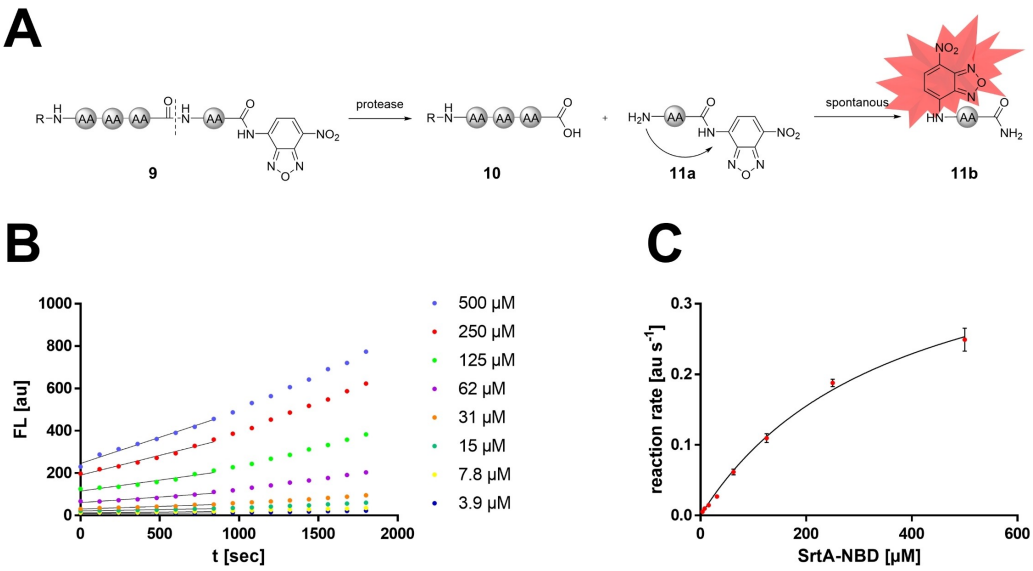


**Figure 5.** Prime site NBD auto-activating substrates as FRET substrate replacement. (A) Schematic depiction of the substrate activation mechanism. Rearrangement of the substrate after cleavage by the protease yields fluorophore activation. (B) Fluorescence progress curves for the conversion of the Bz–Leu–Pro–Ala–Thr–Gly–NBD (7d) substrate by SrtA. (C) Michaelis–Menten plot for the SrtA substrate.

**Table 3.** Enzyme- and substrate-specific kinetic constants for NBD-based and corresponding parent substrates. Michaelis–Menten constant ($K_M$), maximum turnover rate ($v_{max}$), turnover number ($k_{cat}$), catalytic efficiency ($k_{cat}/K_M$).

| protease | NBD substrate | | | | Parent substrate | | | |
|---|---|---|---|---|---|---|---|---|
| | $K_M$ [µM] | $v_{max}$ [nM·min$^{-1}$] | $k_{cat}$ [min$^{-1}$] | $k_{cat}/K_M$ [L·µmol$^{-1}$ min$^{-1}$] | $K_M$ [µM] | $v_{max}$ [nM·min$^{-1}$] | $k_{cat}$ [min$^{-1}$] | $k_{cat}/K_M$ [L·µmol$^{-1}$ min$^{-1}$] |
| Thermolysin | 56.4 ± 4.22 | 52.8 ± 2.3 | 73.1 ± 3.1 | 1.30 ± 0.11 | 703 ± 110 | (3.0 ± 0.3) $10^4$ | (4.2 ± 0.4) $10^4$ | 59.1 ± 10.7 |
| SrtA | 365 ± 35[a] | 156 ± 7 | 0.12 ± 0.01 | (3.28 ± 0.35) $10^{-4}$ | 92.5 ± 9.62 | 459 ± 22 | 0.35 ± 0.02 | 0.0038 ± 0.0004 |
| MMP9 | 26.7 ± 7.70 | 10.3 ± 1.03 | 4.12 ± 0.40 | 0.15 ± 0.05 | 24.7 ± 4.8 | 241 ± 27 | 96.5 ± 10.7 | 3.91 ± 0.88 |

[a] The apparent $K_M$ value of the SrtA FRET substrate is in accordance with the literature value which is distorted by the inner filter effect (Dnp internal quenching). An HPLC-derived $K_M$ value was found to be in the magnitude of $K_M > 1$ mM.[58]

By this, inhibition values were corrected to the zero-substrate concentration, which 1.) allowed the comparison between different substrate affinities and their concentrations; and 2.) showed that the determined $K_M$ values for NBD substrates (Tables 2 and 3) are valid compared to their reported parent substrates. Here, we could show that $K_i$ values of NBD-based and parent substrates differ usually by less than 10% and in some cases by max. a factor of three. It can therefore be assumed that the NBD-based substrates are a well-suitable alternative for fluorometric assays in drug discovery.

## Mitigation of Typical Protease Assay Interferences

The excitation and detection wavelengths of the NBD fluorophore ($\lambda_{ex} = 485$ nm, $\lambda_{em} = 535$ nm) are shifted towards the lower energy range compared to the commonly used AMC substrates ($\lambda_{ex} = 380$ nm, $\lambda_{em} = 460$ nm). In this regard, these assay conditions might be able to suppress the most typical assay interferences, because interfering physicochemical transitions do occur in the near UV-light spectrum.[24,25,27]

Using rhodesain as an example protease with a drug discovery context,[57] we investigated some compounds from our in-house library that are known to lead to false positive results while using the AMC-based rhodesain substrate. By using the newly developed NBD substrate, we aim to reduce these recurring assay interferences (Figure 6 and Figure S48). In this sense, we could show that the apparent inhibition in the AMC-based assay (attenuation of fluorescence increase) is due to common assay interferences, and the NBD-based substrate is not affected. Detailed molecular explanations of the interference effects can be found in the Supporting Information.

## Smartphone-Based Fluorometer for Usage in Classroom Applications

The fluorescence of NBD-based dyes is relatively strong in quantum yield and brightness with the maximum sensitivity in the visible region (see above).[59,60] Thus, NBD substrates are potentially suitable for use with DIY or low-cost Vis-fluorometers to perform kinetic protease studies in classroom-like

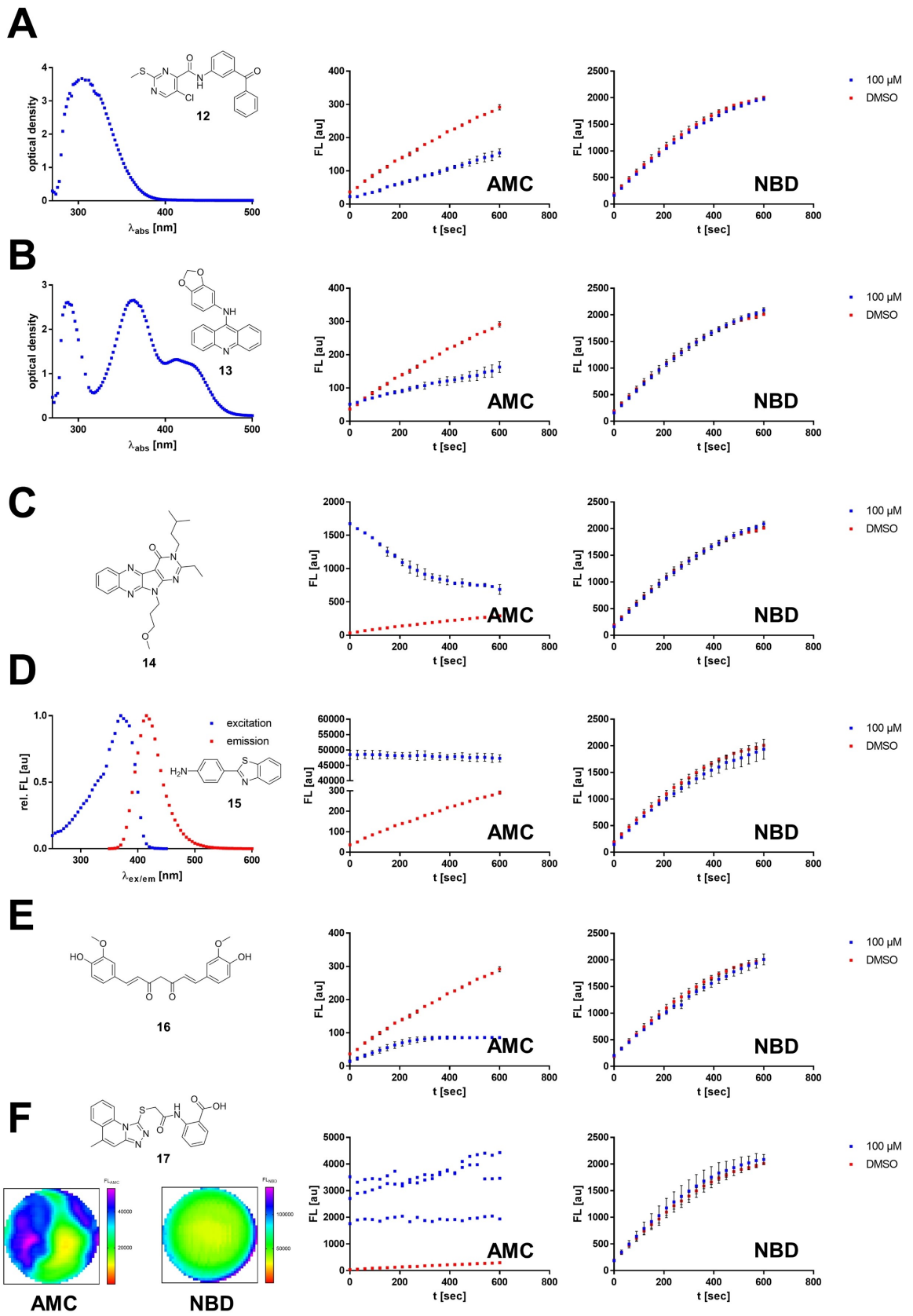


**Figure 6.** Mitigation of typical AMC assay interferences by an NBD substrate. Each interference example was performed for rhodesain assay conditions with the respective AMC and NBD substrate. (A) Inner filter effect of compound 12 (100 µM): compound absorbance spectrum; AMC-based assay; NBD-based assay. (B) Fluorophore quenching by compound 13 (100 µM): compound absorbance spectrum; AMC- and NBD-based assay. (C) Autofluorescence decay of compound 14 (100 µM) (D) Detector non-linearity by compound 15 (100 µM): compound fluorescence spectrum; AMC- and NBD-based assay. (E) Photosensitization of radical oxygen species by compound 16 (100 µM). (F) Reflecting inhibitor aggregates of compound 17 (100 µM): fluorometric well-homogeneity scan with AMC resp. NBD assay wavelengths; AMC- and NBD-based assay.

experiments.[61–63] Previous fluorogenic substrates do not allow for such conceptualizations, as monitoring substrate turnover of AMC and FRET substrates requires an excitation light source in the UV range, which is rarely available in the context of educational activities.

In fact, we were able to show that substrate turnover of Z–Phe–Arg–NBD (500 μM) using the cysteine protease rhodesain (1 μM) is possible by using only a conventional smartphone (Xiaomi Redmi 10) as a detection device (Figure 7). For this purpose, the camera lens and the built-in lamp were covered with LeeFilter films (cost < 10 ct): orange film (2×2 cm, LeeFilters 158 Deep Orange) and blue film (2×2 cm, LeeFilters 120 Deep Blue) as excitation resp. emission filters (Figure 7A). Recording a video of the reaction mixture in a 96-well plate with the built-in camera and analyzing the brightness in the well over time enabled the recording of a substrate turnover curve (Figure 7C and Supporting Information Movie 1).

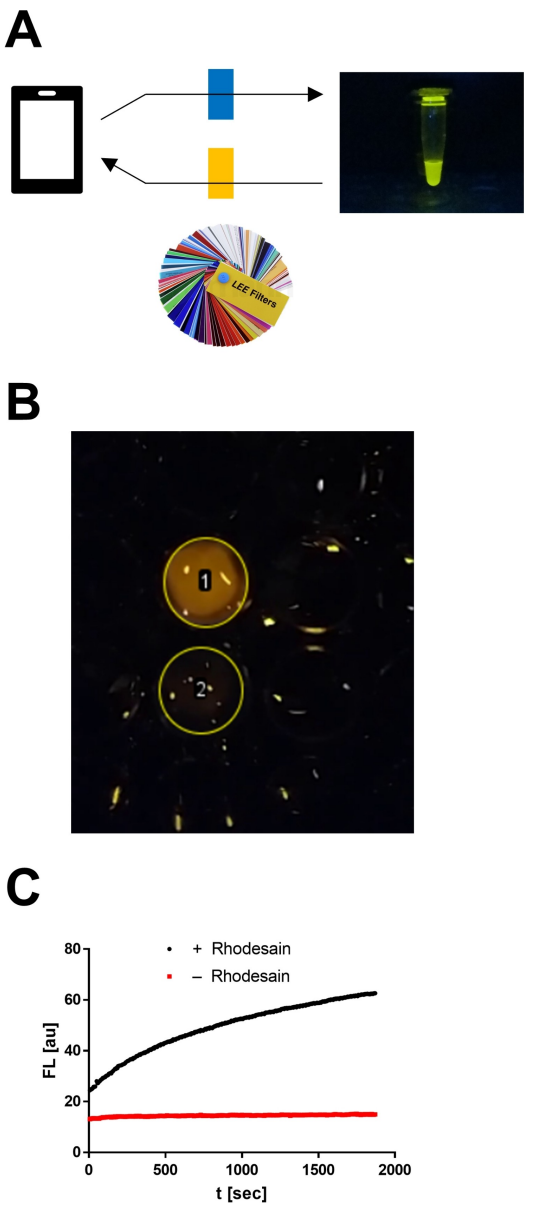


**Figure 7.** Smartphone-based assay for rhodesain activity. (A) Schematic representation of the experimental setup with a fluorescence-enabled photograph of an NBD-$NH_2$ solution (1 mM) in rhodesain assay buffer. (B) Screenshot of a reaction mixture containing rhodesain (1 μM) and the Z–Phe–Arg–NBD substrate (500 μM) in a 96-well plate. Circle 1 highlights a well after the addition of rhodesain enzyme, whereas circle 2 shows only NBD substrate in rhodesain assay buffer. (C) Fluorescence progress curves by analysis of the brightness in the wells (ImageJ 1.53).

## Conclusions

In this study, protease substrates with NBD as a fluorogenic reporter group were designed, synthesized, and tested for utilization in drug discovery applications. Compared to the previous substrate gold standards, the absorption and emission characteristics of NBD are red-shifted to the visible spectrum. In total, we described the synthesis of substrates for 10 different proteases from the cysteine-, serine-, and metalloprotease classes. By this, we were able to obtain substrates for proteases with carboxypeptidase activity (XXX|NBD) as well as for proteases with endopeptidase activity and specificity requirements in the prime site (XX|**X**–NBD). The suitability of the new substrates was confirmed by determining enzyme- and substrate-specific kinetic parameters. The $K_M$ values determined for the NBD-based substrates were in the same order of magnitude as the parent AMC- resp. FRET substrates. Determination of inhibition constants ($K_i$ and $k_{inact}$) of known inhibitors confirmed that NBD substrates are well-suitable for various applications. In this regard, typical medicinal chemistry-related assay interferences such as the inner filter effect, fluorophore quenching, and autofluorescence decay could be avoided by using the NBD substrates. Thus, in summary, NBD substrates may not only provide a suitable alternative to previously used fluorophores but may form the basis of a new generation of fluorometric assays.

## Experimental Section

Fluorometric assays: Fluorometric assays were performed with a Tecan Spark 10 M plate reader using white flat-bottom 96-well microtiter plates from Greiner Bio-One. Measurements were performed in at least three independent technical replicates. Typically, each well contained 180 μL buffer, 5 μL enzyme stock solution, 10 μL inhibitor in DMSO or pure DMSO for mock treatment, and 5 μL solution of the corresponding protease substrate in DMSO, resulting in a total volume of 200 μL (for MMP9: total volume 100 μL, 1 μL substrate, 98 μL buffer, 1 μL enzyme). The fluorescence was measured for 10 min or for 30 min every 30 s with the following excitation and emission wavelengths.

*Emission and Excitation wavelengths.* AMC: $\lambda_{ex} = 380$ nm, $\lambda_{em} = 460$ nm; FAGLA: $\lambda_{abs} = 322$ nm; Abz/Dap(dnp): $\lambda_{ex} = 320$ nm, $\lambda_{em} = 430$ nm; NBD: $\lambda_{ex} = 485$ nm, $\lambda_{em} = 535$ nm; Dnp/Trp: $\lambda_{ex} = 280$ nm, $\lambda_{em} = 360$ nm.

*Enzyme Buffers and Substrates.* **Rhodesain** (enzyme: 1 nM, 50 mM sodium acetate pH 5.5, 5 mM EDTA, 200 mM NaCl, 5 mM DTT, 10 μM Z–Phe–Arg–AMC/10 μM Z–Phe–Arg–NBD); **SARS-CoV 2 $M^{pro}$** (enzyme: 250 nM, 20 mM Tris pH 7.5, 0.1 mM EDTA, 200 mM NaCl, 1 mM DTT, 60 μM Boc–Abu–Tle–Leu–Gln–AMC/30 μM Boc–Abu–Tle–Leu–Gln–NBD); **DENV2 and ZIKV NS2B/NS3** (en-

zyme: 250 nM (DENV) & 25 nM (ZIKV), 50 mM Tris pH 7.5, 100 μM Boc–Gly–Arg–Arg–AMC/50 μM Z–Gly–Arg–Arg–NBD); **Urokinase plasminogen activator (uPA)** (enzyme: 10 U, 50 mM Tris pH 7.4, 50 mM NaCl, 0.5 mM EDTA, 240 μM Z–Gly–Gly–Arg–AMC/10 μM Z–Gly–Gly–Arg–NBD); **Sortase A (SrtA)** (enzyme: 1.3 μM, 50 mM Tris pH 7.5, 150 mM NaCl, 5 mM $CaCl_2$, 0.5 mM $Gly_4$, 25 μM Abz-LPETG-Dap(dnp)-OH/100 μM Bz–Leu–Pro–Ala–Thr–Gly–NBD); **SARS-CoV 2 $PL^{pro}$** (enzyme: 100 nM, 20 mM Tris pH 7.5, 0.1 mM EDTA, 200 mM NaCl, 1 mM DTT, 50 μM Z–Arg–Leu–Arg–Gly–Gly–AMC/40 μM Z–Arg–Leu–Arg–Gly–Gly–NBD); **Cathepsin S (CatS)** (enzyme: 10 nM, enzyme buffer: 35 mM $K_3PO_4$ pH 6.5, 35 mM sodium acetate, 2 mM DTT, 2 mM EDTA, assay buffer: 50 mM $K_3PO_4$ pH 6.5, 2.5 mM DTT, 2.5 mM EDTA, 10 μM Z–Val–Val–Arg–AMC/10 μM Z–Val–Val–Arg–NBD); **Matrixmetalloprotease 9 (MMP9)** (enzyme: 2.5 nM, 150 mM NaCl, 50 mM Tris–HCl pH 7.5, 20 μM $ZnCl_2$, 1 mM $CaCl_2$, Dnp–Pro–Leu–Gly–Met–Trp–Ser–Arg–$NH_2$/40 μM Z–Pro–Leu–Gly–Met–NBD); **Thermolysin** (enzyme: 0.7 nM, 100 mM Tris, 100 mM NaBr, 2.5 mM $CaCl_2$, 100 μM FAGLA/20 μM Bz–Gly–Phe–NBD).

Chemistry: All reagents and solvents were of analytical grade quality and purchased from Sigma-Aldrich, Carbolution, BLDpharm, or FisherScientific. Chemicals were used without further purification. $^1H$ and $^{13}C$ spectra were recorded on a Bruker Fourier 300 or Bruker Avance III 600 using DMSO-$d_6$ or $CDCl_3$, as solvent. Chemical shifts δ are given in parts per million (ppm) using residual proton peaks of the solvent as an internal standard. UV-chromatograms and mass spectra were obtained by LC-MS consisting of an Agilent 1100 series HPLC system using an Agilent Poroshell 120 EC-C18 150×2.10 mm, 4 μm column or an Agilent Zorbax SB Aq. 150× 4.6 mm, 5 μm column. Detection wavelengths were 210, 254, and 396 nm. The tested substrates and inhibitors displayed a purity ≥95% in all cases. The molecular mass was confirmed by an Agilent 1100 series LC/MSD Trap with electron spray ionization (ESI) in positive ionization mode. Melting points (uncorrected) were determined in open capillaries using a Schorpp Gerätetechnik MPM-H3 melting point device. Specific rotations $[\alpha]_D^{20}$ were measured on a P3000 polarimeter from Krüss and are reported in $cm^3\,g^{-1}\,dm^{-1}$. Detailed information on the synthesis and analytical data for characterization of NBD-substrates can be found in the Supporting Information.

## Supporting Information

The authors have cited additional references within the Supporting Information.[27,41,47,52–54,56,64–89]

Additional experimental Procedures (Protein Constructs and Expression, Fluorometric Assay, Molecular Docking, Chemistry) and Results and Discussion (Autocleavage of NS2B/NS3 Protease Substrate, Stability of Substrates, Fluorometric Assay Data).

## Acknowledgements

T.S. acknowledges financial support from the German Research Foundation (DFG), Collaborative Research Center (CRC) SFB 1066 (projects Q5). F.B. acknowledges financial support from the Johannes Gutenberg University of Mainz. Open Access funding enabled and organized by Projekt DEAL.

## Conflict of Interests

The authors declare no conflict of interest.

## Data Availability Statement

The data that support the findings of this study are available in the supplementary material of this article.

**Keywords:** assay interferences · fluorescent probes · medicinal chemistry · nitrobenzofurazane · proteases

[1] S. Udenfriend, in *Fluoresc. Assay Biol. Med.*, Elsevier, **1969**, pp. 1–41.
[2] F. Ciruela, *Curr. Opin. Biotechnol.* **2008**, *19*, 338–343.
[3] T. D. Pollard, *Mol. Biol. Cell* **2010**, *21*, 4061–4067.
[4] M. Leopoldo, E. Lacivita, F. Berardi, R. Perrone, *Drug Discovery Today* **2009**, *14*, 706–712.
[5] H. Maus, G. Hinze, S. J. Hammerschmidt, T. Basché, T. Schirmeister, *Protein Sci.* **2023**, *32*.
[6] C. Götz, G. Hinze, A. Gellert, H. Maus, F. von Hammerstein, S. J. Hammerschmidt, L. M. Lauth, U. A. Hellmich, T. Schirmeister, T. Basché, *J. Phys. Chem. B* **2021**, *125*, 6837–6846.
[7] A. Eatemadi, H. T. Aiyelabegan, B. Negahdari, M. A. Mazlomi, H. Daraee, N. Daraee, R. Eatemadi, E. Sadroddiny, *Biomed. Pharmacother.* **2017**, *86*, 221–231.
[8] P. Müller, H. Maus, S. J. Hammerschmidt, P. M. Knaff, V. Mailänder, T. Schirmeister, C. Kersten, *Curr. Med. Chem.* **2022**, *29*, 635–665.
[9] C. López-Otín, J. S. Bond, *J. Biol. Chem.* **2008**, *283*, 30433–30437.
[10] G. Abbenante, D. Fairlie, *Med. Chem.* **2005**, *1*, 71–104.
[11] P. D. Leeson, A. P. Bento, A. Gaulton, A. Hersey, E. J. Manners, C. J. Radoux, A. R. Leach, *J. Med. Chem.* **2021**, *64*, 7210–7230.
[12] Y. N. Lamb, *Drugs* **2022**, *82*, 585–591.
[13] M. Drag, G. S. Salvesen, *Nat. Rev. Drug Discovery* **2010**, *9*, 690–701.
[14] B. Turk, *Nat. Rev. Drug Discovery* **2006**, *5*, 785–799.
[15] V. Canbay, U. auf dem Keller, *Curr. Opin. Chem. Biol.* **2021**, *60*, 89–96.
[16] I. L. H. Ong, K.-L. Yang, *Analyst* **2017**, *142*, 1867–1881.
[17] A. Carmel, M. Zur, A. Yaron, E. Katchalski, *FEBS Lett.* **1973**, *30*, 11–14.
[18] H. Tuppy, U. Wiesbauer, E. Wintersberger, *Hoppe-Seyler's Z. Physiol. Chem.* **1962**, *329*, 278–288.
[19] M. Zimmerman, E. Yurewicz, G. Patel, *Anal. Biochem.* **1976**, *70*, 258–262.
[20] S. Markossian, A. Grossman, K. Brimacombe, M. Arkin, D. Auld, C. Austin, J. Baell, T. Chung, N. P. Coussens, J. L. Dahlin, *Assay Guidance Manual*, Eli Lilly & Company and The National Center For Advancing Translational Sciences, **2004**.
[21] B. C. Chenna, L. Li, D. M. Mellott, X. Zhai, J. L. Siqueira-Neto, C. Calvet Alvarez, J. A. Bernatchez, E. Desormeaux, E. Alvarez Hernandez, J. Gomez, J. H. McKerrow, J. Cruz-Reyes, T. D. Meek, *J. Med. Chem.* **2020**, *63*, 3298–3316.
[22] T. T. Baird, C. S. Craik, in *Handb. Proteolytic Enzym.*, **2013**, pp. 2594–2600.
[23] A. Jadhav, R. S. Ferreira, C. Klumpp, B. T. Mott, C. P. Austin, J. Inglese, C. J. Thomas, D. J. Maloney, B. K. Shoichet, A. Simeonov, *J. Med. Chem.* **2010**, *53*, 37–51.
[24] J. Comley, *Drug Discov. World Summer 2003* **2003**, *4*, 91–98..
[25] S. K. Grant, J. G. Sklar, R. T. Cummings, *SLAS Discov.* **2002**, *7*, 531–540.
[26] Y. Liu, W. Kati, C.-M. Chen, R. Tripathi, A. Molla, W. Kohlbrenner, *Anal. Biochem.* **1999**, *267*, 331–335.
[27] N. Thorne, D. S. Auld, J. Inglese, *Curr. Opin. Chem. Biol.* **2010**, *14*, 315–324.
[28] F. E. Jernigan, D. S. Lawrence, *Chem. Commun.* **2013**, *49*, 6728.
[29] J.-M. Delaissé, Y. Eeckhout, G. Vaes, *Biochem. Biophys. Res. Commun.* **1984**, *125*, 441–447.
[30] S. G. Deeks, M. Smith, M. Holodniy, J. O. Kahn, *J. Am. Med. Assoc.* **1997**, *277*, 145–153.
[31] S. Jo, H. Kim, S. Kim, D. H. Shin, M. Kim, *Chem. Biol. Drug Des.* **2019**, *94*, 2023–2030.
[32] C. Jiang, H. Huang, X. Kang, L. Yang, Z. Xi, H. Sun, M. D. Pluth, L. Yi, *Chem. Soc. Rev.* **2021**, *50*, 7436–7495.
[33] K. Okada, T. Yamaguchi, K. Dodo, M. Sodeoka, S. Obika, *Bioorg. Med. Chem.* **2019**, *27*, 1444–1448.

[34] Y. Xie, L. Chen, R. Wang, J. Wang, J. Li, W. Xu, Y. Li, S. Q. Yao, L. Zhang, Q. Hao, H. Sun, *J. Am. Chem. Soc.* **2019**, *141*, 18428–18436.
[35] M. He, Z. Han, J. Qiao, L. Ngo, M. P. Xiong, Y. G. Zheng, *Chem. Commun.* **2018**, *54*, 5594–5597.
[36] I. N. Gober, M. L. Waters, *J. Am. Chem. Soc.* **2016**, *138*, 9452–9459.
[37] Y. Xie, J. Ge, H. Lei, B. Peng, H. Zhang, D. Wang, S. Pan, G. Chen, L. Chen, Y. Wang, Q. Hao, S. Q. Yao, H. Sun, *J. Am. Chem. Soc.* **2016**, *138*, 15596–15604.
[38] J. M. An, S. Kang, E. Huh, Y. Kim, D. Lee, H. Jo, J. F. Joung, V. J. Kim, J. Y. Lee, Y. S. Dho, Y. Jung, J. K. Hur, C. Park, J. Jung, Y. Huh, J.-L. Ku, S. Kim, T. Chowdhury, S. Park, J. S. Kang, M. S. Oh, C.-K. Park, D. Kim, *Chem. Sci.* **2020**, *11*, 5658–5668.
[39] D. Castagnolo, M. Pagano, M. Bernardini, M. Botta, *Tetrahedron Lett.* **2012**, *53*, 5008–5011.
[40] P. M. Knaff, P. Müller, C. Kersten, L. Wettstein, J. Münch, K. Landfester, V. Mailänder, *Biomacromolecules* **2022**, *23*, 2236–2242.
[41] Y. Yang, D. Zhang, M. Xu, J. Wang, J. Chen, L. Wang, *Monatsh. Chem.* **2018**, *149*, 1003–1008.
[42] L. F. Bernal-Perez, L. Prokai, Y. Ryu, *Anal. Biochem.* **2012**, *428*, 13–15.
[43] P. B. Ghosh, M. W. Whitehouse, *Biochem. J.* **1968**, *108*, 155–156.
[44] S. Jung, N. Fuchs, C. Grathwol, U. A. Hellmich, A. Wagner, E. Diehl, T. Willmes, C. Sotriffer, T. Schirmeister, *Eur. J. Med. Chem.* **2022**, *238*, 114460.
[45] D. Dana, A. R. Davalos, S. De, P. Rathod, R. K. Gamage, J. Huestis, N. Afzal, Y. Zavlanov, S. S. Paroly, S. A. Rotenberg, G. Subramaniam, K. J. Mark, E. J. Chang, S. Kumar, *Bioorg. Med. Chem.* **2013**, *21*, 2975–2987.
[46] W. Rut, K. Groborz, L. Zhang, X. Sun, M. Zmudzinski, B. Pawlik, X. Wang, D. Jochmans, J. Neyts, W. Młynarski, R. Hilgenfeld, M. Drag, *Nat. Chem. Biol.* **2021**, *17*, 222–228.
[47] F. Barthels, G. Marincola, T. Marciniak, M. Konhäuser, S. Hammerschmidt, J. Bierlmeier, U. Distler, P. R. Wich, S. Tenzer, D. Schwarzer, W. Ziebuhr, T. Schirmeister, *ChemMedChem* **2020**, *15*, 839–850.
[48] A. Narayanan, M. Narwal, S. A. Majowicz, C. Varricchio, S. A. Toner, C. Ballatore, A. Brancale, K. S. Murakami, J. Jose, *Commun. Biol.* **2022**, *5*, 169.
[49] A. Dal Corso, M. Catalano, A. Schmid, J. Scheuermann, D. Neri, *Angew. Chem.* **2018**, *130*, 17424–17428.
[50] H. Lai, G. Sridhar Prasad, R. Padmanabhan, *Antiviral Res.* **2013**, *97*, 74–80.
[51] H. Maus, F. Barthels, S. J. Hammerschmidt, K. Kopp, B. Millies, A. Gellert, A. Ruggieri, T. Schirmeister, *Bioorg. Med. Chem.* **2021**, *47*, 116392.
[52] S. Netzel-Arnett, S. K. Mallya, H. Nagase, H. Birkedal-Hansen, H. E. Van Wart, *Anal. Biochem.* **1991**, *195*, 86–92.
[53] P. A. Bartlett, C. K. Marlowe, *Biochemistry* **1987**, *26*, 8553–8561.
[54] S. M. Khan, D. W. Darnall, *Anal. Biochem.* **1978**, *86*, 332–336.
[55] D. J. Murphy, *Anal. Biochem.* **2004**, *327*, 61–67.
[56] T. Schirmeister, J. Kesselring, S. Jung, T. H. Schneider, A. Weickert, J. Becker, W. Lee, D. Bamberger, P. R. Wich, U. Distler, S. Tenzer, P. Johé, U. A. Hellmich, B. Engels, *J. Am. Chem. Soc.* **2016**, *138*, 8332–8335.
[57] R. Ettari, S. Previti, L. Tamborini, G. Cullia, S. Grasso, M. Zappalà, *Mini-Rev. Med. Chem.* **2016**, *16*, 1374–1391.
[58] R. G. Kruger, P. Dostal, D. G. McCafferty, *Anal. Biochem.* **2004**, *326*, 42–48.
[59] S. Uchiyama, T. Santa, T. Fukushima, H. Homma, K. Imai, *J. Chem. Soc. Perkin Trans. 2* **1998**, 2165–2174.
[60] B. E. Tebikachew, F. Edhborg, N. Kann, B. Albinsson, K. Moth-Poulsen, *Phys. Chem. Chem. Phys.* **2018**, *20*, 23195–23201.
[61] M. A. Hossain, J. Canning, S. Ast, T. L. Yen, P. Rutledge, A. Jamalipour, in *Adv. Photonics*, OSA, Washington, D. C., **2014**, p. SeTh2 C.1.
[62] L. M. Azad, H. Ehtesabi, A. Rezaei, *Nano-Struct.Nano-Objects* **2021**, *26*, 100722.
[63] A. Jamalipour, M. A. Hossain, **2019**, pp. 15–36.
[64] G. Amendola, R. Ettari, S. Previti, C. Di Chio, A. Messere, S. Di Maro, S. J. Hammerschmidt, C. Zimmer, R. A. Zimmermann, T. Schirmeister, M. Zappalà, S. Cosconati, *J. Chem. Inf. Model.* **2021**, *61*, 2062–2073.
[65] B. Millies, F. Von Hammerstein, A. Gellert, S. Hammerschmidt, F. Barthels, U. Göppel, M. Immerheiser, F. Elgner, N. Jung, M. Basic, C. Kersten, W. Kiefer, J. Bodem, E. Hildt, M. Windbergs, U. A. Hellmich, T. Schirmeister, *J. Med. Chem.* **2019**, *62*, 11359–11382.
[66] L. Schmohl, J. Bierlmeier, N. von Kügelgen, L. Kurz, P. Reis, F. Barthels, P. Mach, M. Schutkowski, C. Freund, D. Schwarzer, *Bioorg. Med. Chem.* **2017**, *25*, 5002–5007.
[67] Y. M. Báez-Santos, S. J. Barraza, M. W. Wilson, M. P. Agius, A. M. Mielech, N. M. Davis, S. C. Baker, S. D. Larsen, A. D. Mesecar, *J. Med. Chem.* **2014**, *57*, 2393–2412.
[68] J. Joossens, P. Van der Veken, G. Surpateanu, A.-M. Lambeir, I. El-Sayed, O. M. Ali, K. Augustyns, A. Haemers, *J. Med. Chem.* **2006**, *49*, 5785–5793.
[69] B. J. Buckley, A. Aboelela, E. Minaei, L. X. Jiang, Z. Xu, U. Ali, K. Fildes, C.-Y. Cheung, S. M. Cook, D. C. Johnson, D. A. Bachovchin, G. M. Cook, M. Apte, M. Huang, M. Ranson, M. J. Kelso, *J. Med. Chem.* **2018**, *61*, 8299–8320.
[70] A. Welker, C. Kersten, C. Müller, R. Madhugiri, C. Zimmer, P. Müller, R. Zimmermann, S. Hammerschmidt, H. Maus, J. Ziebuhr, C. Sotriffer, T. Schirmeister, *ChemMedChem* **2021**, *16*, 340–354.
[71] D. Brömme, *Curr. Protoc. Protein Sci.* **2000**, *21*.
[72] R. A. Friesner, J. L. Banks, R. B. Murphy, T. A. Halgren, J. J. Klicic, D. T. Mainz, M. P. Repasky, E. H. Knoll, M. Shelley, J. K. Perry, D. E. Shaw, P. Francis, P. S. Shenkin, *J. Med. Chem.* **2004**, *47*, 1739–1749.
[73] G. N. Lewis, M. Calvin, *Chem. Rev.* **1939**, *25*, 273–328.
[74] L. D. Dias, K. C. Blanco, I. S. Mfouo-Tynga, N. M. Inada, V. S. Bagnato, *J. Photochem. Photobiol. C* **2020**, *45*, 100384.
[75] I. Ahmad, S. Ahmed, Z. Anwar, M. A. Sheraz, M. Sikorski, *Int. J. Photoenergy* **2016**, *2016*, 1–19.
[76] K. T. Kazantzis, K. Koutsonikoli, B. Mavroidi, M. Zachariadis, P. Alexiou, M. Pelecanou, K. Politopoulos, E. Alexandratou, M. Sagnou, *Photochem. Photobiol. Sci.* **2020**, *19*, 193–206.
[77] K. M. Nelson, J. L. Dahlin, J. Bisson, J. Graham, G. F. Pauli, M. A. Walters, *J. Med. Chem.* **2017**, *60*, 1620–1637.
[78] D. Steverding, *Molecules* **2019**, *25*, 143.
[79] S. Ludewig, M. Kossner, M. Schiller, K. Baumann, T. Schirmeister, *Curr. Top. Med. Chem.* **2010**, *10*, 368–382.
[80] Lord Rayleigh, *Lond. Edinb. Dublin Philos. Mag. J. Sci.* **1881**, *12*, 81–101.
[81] S. Jung, N. Fuchs, P. Johe, A. Wagner, E. Diehl, T. Yuliani, C. Zimmer, F. Barthels, R. A. Zimmermann, P. Klein, W. Waigel, J. Meyr, T. Opatz, S. Tenzer, U. Distler, H.-J. Räder, C. Kersten, B. Engels, U. A. Hellmich, J. Klein, T. Schirmeister, *J. Med. Chem.* **2021**, *64*, 12322–12358.
[82] R. D. A. Wilkinson, A. Young, R. E. Burden, R. Williams, C. J. Scott, *Mol. Cancer* **2016**, *15*, 29.
[83] L. Fu, S. Shao, Y. Feng, F. Ye, X. Sun, Q. Wang, F. Yu, Q. Wang, B. Huang, P. Niu, X. Li, C. C. L. Wong, J. Qi, W. Tan, G. F. Gao, *mBio* **2021**, *12*.
[84] S. Previti, R. Ettari, E. Calcaterra, C. Di Chio, R. Ravichandran, C. Zimmer, S. Hammerschmidt, A. Wagner, M. Bogacz, S. Cosconati, T. Schirmeister, M. Zappalà, *ACS Med. Chem. Lett.* **2022**, *13*, 1083–1090.
[85] M. A. Abduraman, M. Hariono, R. Yusof, N. A. Rahman, H. A. Wahab, M. L. Tan, *Heliyon* **2018**, *4*, e01023.
[86] K. H. Nam, *J. Inorg. Biochem.* **2021**, *215*, 111319.
[87] M. Johansson, A. J. Brooks, D. A. Jans, S. G. Vasudevan, *J. Gen. Virol.* **2001**, *82*, 735–745.
[88] F. Hammerstein, L. M. Lauth, S. Hammerschmidt, A. Wagner, T. Schirmeister, U. A. Hellmich, *FEBS Lett.* **2019**, *593*, 2204–2213.
[89] C. R. Caffrey, E. Hansell, K. D. Lucas, L. S. Brinen, A. Alvarez Hernandez, J. Cheng, S. L. Gwaltney, W. R. Roush, Y.-D. Stierhof, M. Bogyo, D. Steverding, J. H. McKerrow, *Mol. Biochem. Parasitol.* **2001**, *118*, 61–73.

Manuscript received: June 12, 2023
Accepted manuscript online: June 14, 2023
Version of record online: July 28, 2023